# Hardware Implementation of Bidirectional Full Bridge Isolated DC- DC Converter

Miss.S.Srinithi
PG Student,
Department of EEE,
Kathir College of Engineering,
Coimbatore.
nithi266@gmail.com

Dr.B.Vaikundaselvan
Professor & Head,
Department of EEE,
Kathir College of Engineering,
Coimbatore.
vaikungth@yahoo.co.in

Mrs.S.N.Sathya,
Associate Professor,
Department of EEE,
Kathir College of Engineering,
Coimbatore.
sathya.karishni@rediffmail.com

Mr.C. Sivan Raj
Assisant Professor,
Department of EEE,
Kathir College of Engineering,
Coimbatore.
reachsivanraj@gmail.com

*Abstract* — **This paper presents the design and development of an ultra-high efficiency bidirectional isolated full bridge DC-DC converter. To achieve ultra-high efficiency, synchronous rectification and high efficiency magnetics are used. The proposed bidirectional converter allows a power flow in both directions using the same power components; this increases power density and reduce the cost. The converter operates at a switching frequency of 50 kHz with a voltage of 130 volts at one side and 52 volts at the other side of the converter. The fast switching speeds of the switching devices are utilized to achieve extremely high conversion efficiency thus reducing the total volume of the converter. The high power DC-DC converter has attained an extremely high efficiency of 80% in both the directions. The performance of a 1.7 kW bidirectional converter is validated in both forward direction (buck mode) and backward direction (boost mode) using MATLAB simulation.**

**Keywords**— ***DC-DC Converter, Switching Device, buck mode, high efficiency, switching speeds.***

## I. INTRODUCTION

Bidirectional DC-DC converters are used in applications where bidirectional power flow may be required. In Hybrid Electric Vehicles (HEVs) and Electric Vehicles (EVs), these bidirectional converters charge a low voltage (12 V) battery during normal operation (buck mode) and charge or assist the high-voltage (400V/600V) battery or bus in emergency situations like when a high-voltage battery has discharged to a very low energy or capacity level (boost mode). A typical system consists of a full-bridge power stage on the High-Voltage (HV) side, which is isolated from a full-bridge or a current-fed push-pull stage on the Low Voltage (LV) side.

The world's rapidly expanding population and increasing levels of consumerism have given rise to significant environmental issues that must be confronted. Firstly, there is a great reliance on fossil fuels to provide energy, of which a large part is consumed by transportation systems. While shale oil recovery by the hydraulic fracturing process has provided a temporary increase in production, it is only extending the point in time at which demand exceeds supply.

The second, and interrelated, major problem is that of environmental damage in general, and specifically that of air pollution. Aside from the contentious issue of global warming, there is a requirement for a reduction in the burning of hydrocarbons to achieve adequate air quality. The basis for a solution to both problems is in the sustainable use of resources, and considerable effort is being expended investigating forms of renewable, or green, energy [Kaminski.N, 2009]. Two of the more promising alternative energy sources are from wind and solar farms.

These allow for distributed and localized generation, which offers the advantages of reduced distribution costs and improved network security. However, the supply of energy from these sources is variable in nature, due to the dependency on the weather conditions, and results in grid planning and stability issues. Furthermore, the problems caused by these source variations are exacerbated by the wide variations in electrical energy demand, even on an hourly basis within modern societies. Electric vehicles (EVs) are a part of the solution to the energy problem.

Silicon has been used as a power semiconductor material for many decades. The material properties of Silicon have reached its maximum theoretical limit. For power devices, wide band gap materials such as Silicon carbide (SiC) and Gallium Nitride (GaN) are also promising because of their high switching speed and lower switching Figure of Merit (FOM), QossxRDS(ON). Compared to conventional silicon devices, for the same breakdown voltage, GaN devices have smaller area for the same on-resistance.

This paper presents a novel bi-directional isolated DC-DC converter which may be used in the $V_2G$ or DG applications discussed above. It has hardware that is similar to that of a Conventional Dual Active Bridge Converter (CDAB), except that the latter's inductor is replaced with a resonant network to reduce the converter's conduction losses.

## II. BIDIRECTIONAL DC-DC CONVERTER

A PSFB converter consists of four power electronic switches (like MOSFETs or IGBTs) that form a full bridge on the primary side of the isolation transformer and diode rectifiers or MOSFET switches for Synchronous Rectification (SR) on the secondary side. This topology let's all the switching devices to switch with Zero-Voltage Switching (ZVS), resulting in lower switching losses and an efficient converter.

For such an isolated topology, signal rectification is required on the secondary side. For systems with low output voltage and/or high-output current ratings, implementing synchronous rectification achieves the best performance by avoiding diode rectification losses. In this work, synchronous rectification is implemented on the secondary side with various switching schemes to achieve optimum performance under varying load conditions. The circuit

diagram for an isolated bidirectional full bridge DC-DC converter is shown in Fig. 1.

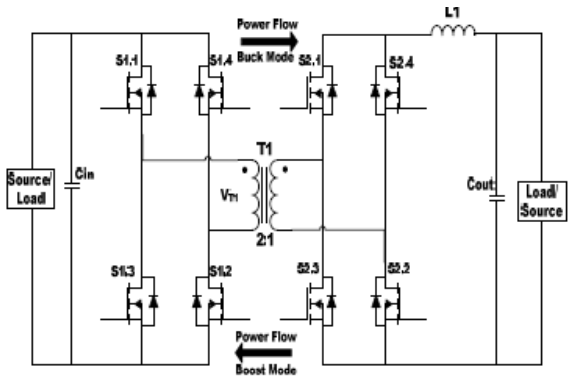


**Fig. 1 Isolated Full Bridge Bidirectional DC-DC Converter**

*A. Buck Mode of Operation*

A DC-DC converter system can be controlled in various modes like Voltage Mode Control (VMC), Average Current Mode Control (ACMC), or peak Current Mode Control (PCMC). Implementing these different control modes for controlling the same power stage typically requires redesigning the control circuit along with some changes to the power stage sensing circuitry.

With a microcontroller-based system, all these modes can be experimented with on the same design with minimal or no additional changes. Fig. 2 shows a simplified circuit of a phase-shifted full bridge. MOSFET switches Q1, Q2, Q3, and Q4 form the full bridge on the primary side of the T1 transformer. Q1 and Q4 are switched at 50% duty and 180 degrees out of phase with each other.

QC and QD are switched at 50% duty and 180 degrees out of phase with each other. The PWM switching signals for leg Q2–Q3 of the full bridge are phase-shifted with respect to those for leg Q1–Q4. The amount of this phase shift decides the amount of overlap between diagonal switches, which decides the amount of energy transferred. D5 and D6 provide diode rectification on the secondary, while Lo and Co form the output filter.

*B. Boost mode of Operation*

The synchronous rectifier switches are the push-pull switches in boost mode. The buck mode output inductor acts as a current source in this mode letting this topology work as a current-fed push-pull converter. Full-bridge switches on the HV side may be kept off and their body diodes used for rectification. The full-bridge switches are used for active rectification in the boost mode.

The push-pull switches are driven with PWM signals with greater than 50% duty cycles that are 180 degrees out of phase with each other. • **t0 – t1:** During this time, Q5 and Q6 are on simultaneously. The inductive energy in the low-voltage winding of the transformer and that in the boost inductor (L1) increases.

• **t1 – t2:** At t1, Q6 is turned off and the stored inductive energy on the LV side is transferred to the HV side through diodes D1 and D3.

The operation during t2–t3 is the same as t0–t1, while that during t3–t4 is similar to t1–t2, except that Q5 is turned off at t3 and diodes D2 and D4 conduct on the HV side.

In this mode of operation, the amount of energy transferred to the HV side is decided by the duty cycle of the signals driving switches Q5 and Q6. Unlike the phase-controlled buck mode, this is a duty-controlled operation.

## III. DESIGN PROCEDURE

*A. Buck Mode*

The operational waveform of the converter in buck mode is presented in Fig. 2. The output voltage, $V_O$ can be expressed in terms of input voltage $V_{in}$ in a buck mode of operation as,

$$V_o = 2n_c D_c V_{in} \quad (1)$$

Where, $n_c$ is the ratio of number of winding turns in low voltage side to number of winding turns in high voltage side. $D_c$ is the duty cycle of the switches in the high voltage side.

*B. Boost Mode*

The operational waveform of the converter in boost mode is shown in Fig. 2. The output voltage, $V_O$ can be expressed in terms of input voltage $V_{in}$ in a boost mode of operation can be expressed as,

$$V_o = \frac{V_d}{1 - D_d} V_{in} \quad (2)$$

Where, $n_c = 1/ n_d$. $D_d$ is the duty cycle of the switches in the low voltage side. $D_d = 1\text{-}D_c$. The output voltage in boost mode operation can be also written as,

$$V_o = \frac{1}{n_c D_c} V_{in} \quad (3)$$

*C. Transformer*

Copper foils are efficiently interleaved to reduce the AC-resistance and thus also reduces the leakage inductance of the transformer. The efficiency of the transformer alone is 99.75%. Eqn. 1, 2 and 3 shows the calculation for the leakage inductance and the AC resistance of the transformer referred to the high voltage side [Nymand.M, 2010].

$$L_{LK} = \mu_0 \frac{n^2 lw}{m^2 bw} \left[\frac{1}{3}\sum hp + \sum h\Delta\right] \quad (4)$$

where, $\mu_0$ is the permeability of free space, N is the number of turns, M is the number of primary–secondary intersections, $l_w$ is the mean turn length, $b_w$ is the breadth of winding, $h_p$ is the height of $p^{th}$ winding portion and $h\Delta$ is the height of primary-secondary intersection is,

$$R_{ac} = R_{dc}\left(\varphi\frac{\sinh 2\varphi + \sin\varphi}{\cosh 2\varphi - \cos\varphi} + \frac{2(m^2-1)}{3}\varphi\frac{\sinh\varphi - \sin\varphi}{\cosh\varphi + \cos\varphi}\right) \quad (5)$$

Where $\varphi=h/\delta$, h is the height of the conductor, $\delta$ is the penetration depth, $R_{ac}$ is the AC resistance of the winding, $R_{dc}$ is the DC resistance and m is the number of layers in the winding. The AC resistance and leakage inductance of the transformer referred to high voltage side is measured using Key sight 4294A precision impedance analyzer.

*D. GaN Devices*

GaN FETs are used at both the high voltage and low voltage sides of the converter. EPC2010C with a breakdown voltage of 200V is used at the high voltage side. EPC2001C are used at the low voltage sides, they have a breakdown voltage of 100V. Four GaN FETs are paralleled in each switch in the topology.

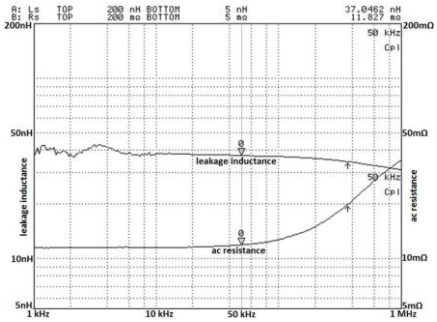


**Fig.2 Measured Value of Transformer AC-Resistance and Leakage Inductance Referred to High Voltage Side**

The maximum gate source voltage for the EPC GaN FET is 6V, which is low compared to the conventional Si MOSFET. The gate threshold voltage of these devices is also small in the range of 1 to 1.5V. So driving of these devices requires special consideration in terms of the drivers used and the PCB design layout.

## IV. RESULT AND DISCUSSION

The Simulink model of the 1.7 kW isolated bidirectional DC-DC converter is shown in Fig. 3. When the efficiency becomes higher, for e.g. above 95%, extensive care has to be taken to measure the efficiency accurately and precisely. Compared to precise voltage measurement, measurement of current is always critical. In this efficiency measurement, current at both input and output side of the converter is measured using current sense resistors. The Simulation parameters are tabulated in Table 1.

**Table 1 Simulation Parameters**

| | |
|---|---|
| **Input Voltage** | 130V |
| **MOSFET** | $R_{on}$=0.1 $R_d$=0.01 |
| **Load** | DC Machine (Permanent Magnet) |
| **Resistance** | 9.94 ohm |

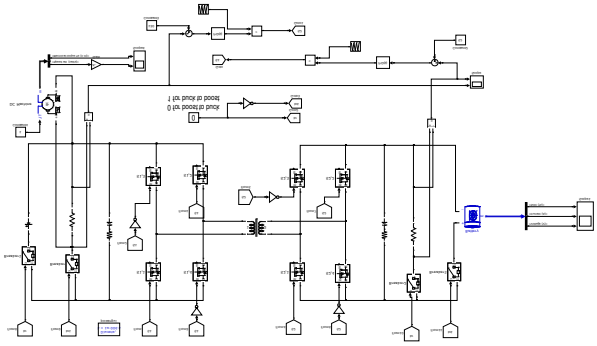

**Fig.3 Simulation Diagram of Bidirectional DC-DC Converter**

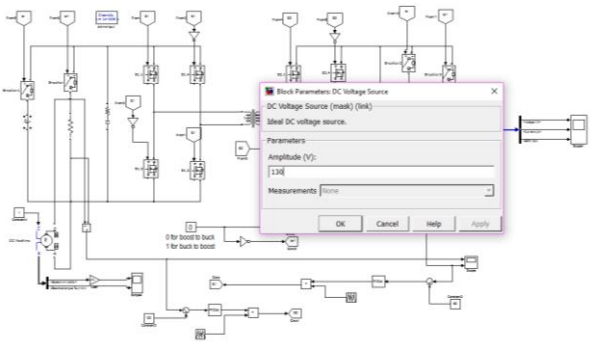

**Fig.4 Input DC Voltage Source 130V**

The buck mode operation of the DC-DC converter is verified by connecting a DC voltage source to the low voltage side of the converter. The high voltage side of the converter is connected to an electric load.

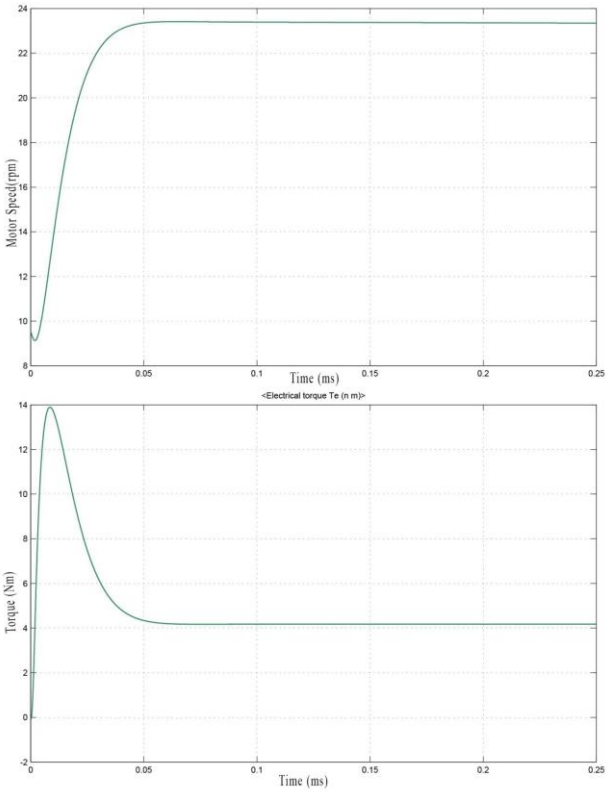


**Fig. 5 Motor Speed and Torque**

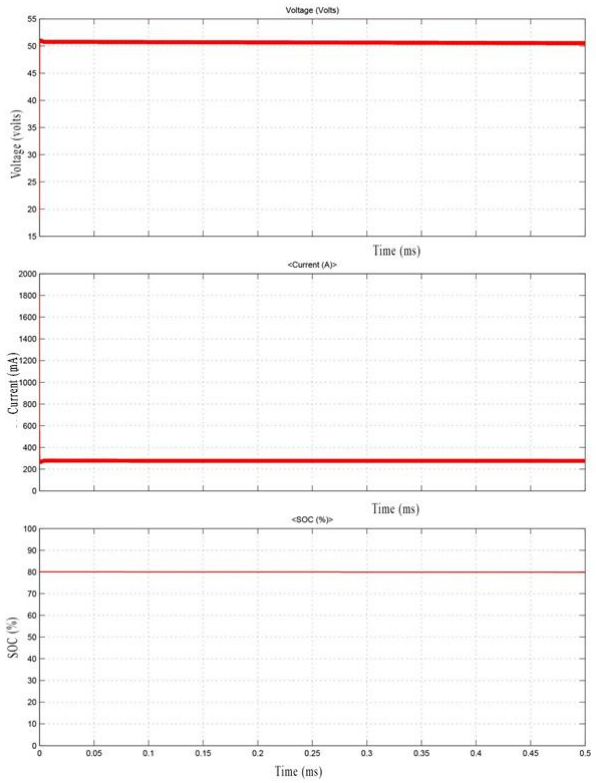


**Fig. 6 Load Voltage, Current and Efficiency**

Fig. 5, 6 and 7 shows the various waveforms of the converter working in forward direction. The measured efficiency of the converter in buck mode is also presented in Fig. 5. The peak efficiency of the converter in buck mode is measured as 80%.

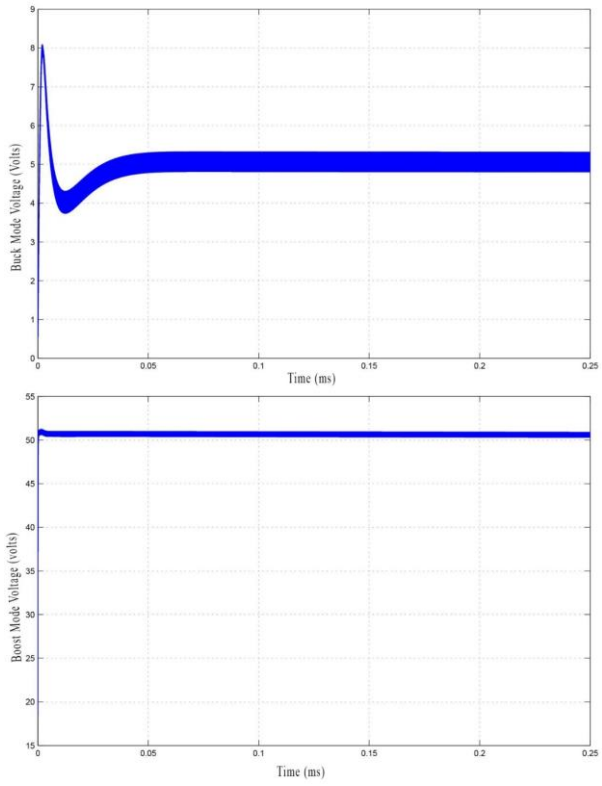


**Fig. 7 Buck and Boost Voltage**

The boost mode operation of the DC-DC converter is verified by applying an input voltage of 52V. The high voltage side of the converter is connected to an external load.

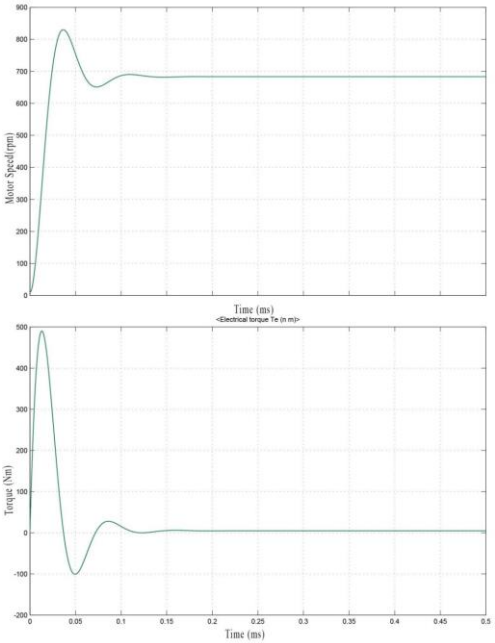


**Fig.8 Motor Speed and Torque in Boost Mode**

Various waveforms of the converter working in backward direction are shown in Fig. 8, 9 and 10. The measured efficiency of the converter in boost mode is also shown in Fig.6; the output power is shown as negative in the efficiency curve. The maximum measured efficiency of the converter is 80%.

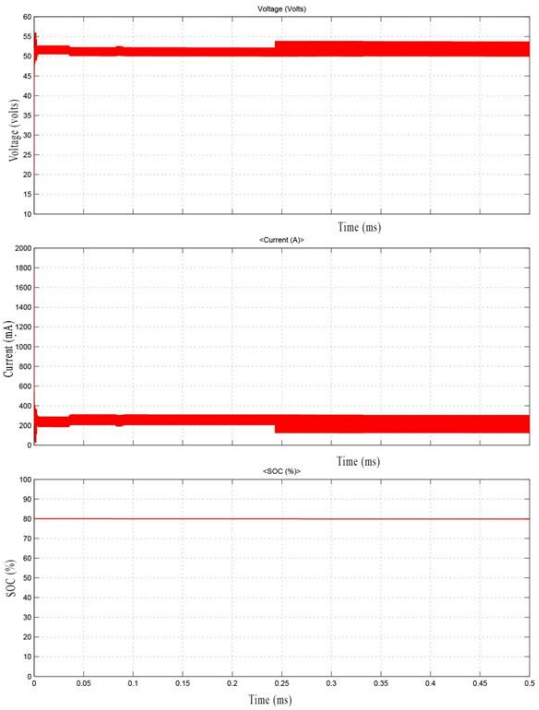


**Fig. 9 Load Voltage, Current and Efficiency in Boost Mode**

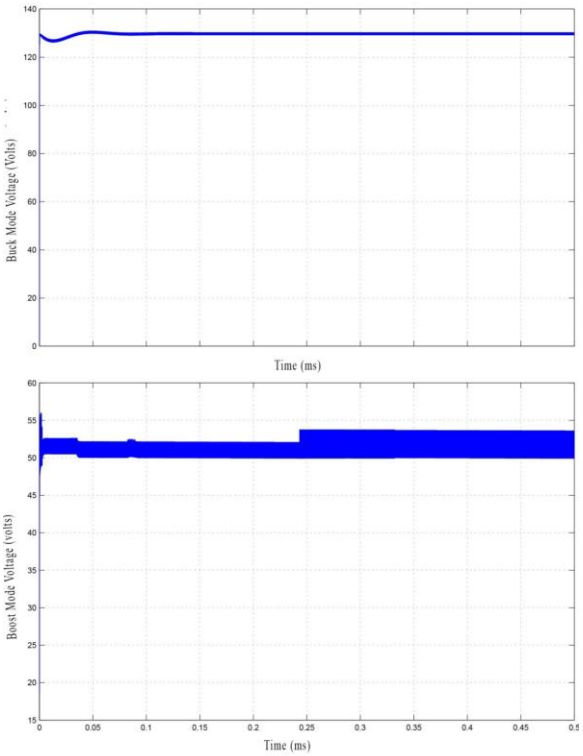


**Fig. 10 Buck and Boost Voltage in Boost Mode**

**Fig. 11 Hardware Design for Proposed Bidirectional Full Bridge Isolated DC-DC Converter**

The hardware design for proposed bidirectional full bridge isolated DC-DC converter is as shown in Fig. 11. The hardware descriptions are,

- The experimental prototype with the proposed configuration is shown in Fig. 11.
- A battery module working at the low-voltage side is employed as an energy-storage element, whose voltage rating is 12 Volts.
- 180W DC motor is used as a load whose rating is 12V, 1500 RPM.
- High frequency 2:1 transformer is used and the voltage range of a step down transformer is 0-15V and the rated current is 1A.
- Regulated Power Supply (RPS) unit is used for the prototype in order to unregulated AC into a constant DC whose range is 0-5V.
- The MOSFET is named as $S_1$,$S_2$,$S_3$,$S_4$ and the FCA76N60N is used
- The inductance value of the output filter is denoted as $L_{out}$ and the value of the inductance is 10 µH.
- The diodes are named as $D_1$, $D_2$, $D_3$, $D_4$ and the device name is RHRP3060.

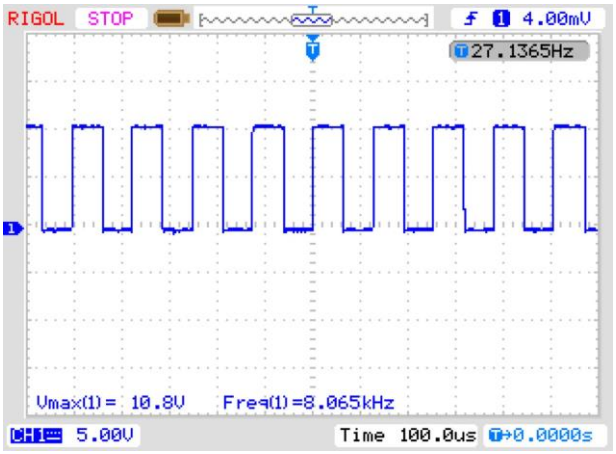


**Fig. 12 Inverter Board's Gate Pulse - Inverter pulse (Forward)**

Fig. 12 and 13 shows the output result for inverter gate pulse and non-inverter pulse in forward direction

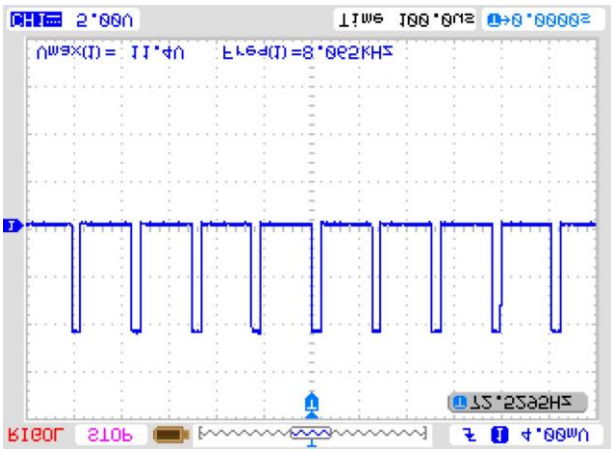

**Fig. 13 Inverter Board's Gate Pulse – Non-Inverter pulse (Forward)**

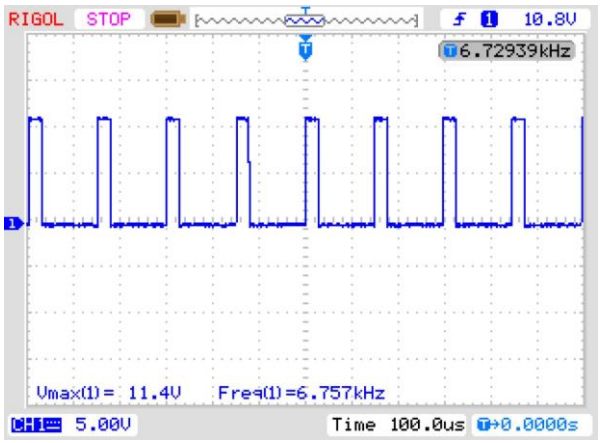


**Fig. 14 Reverse Voltage - Inverter Pulse**

The reverse voltage for inverter pulse and non-inverter pulse is as shown in Fig. 14 and 15.

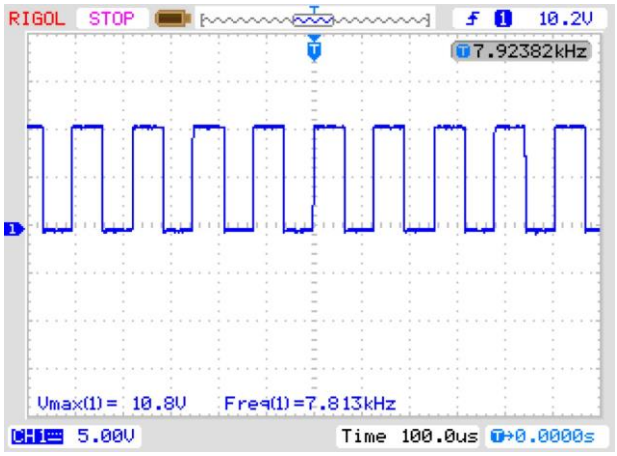


**Fig. 15 Reverse Voltage - Non-Inverter Pulse**

### A. CONCLUSION

An ultra- high efficiency bidirectional isolated DC-DC converter was designed using MATLAB simulation and the hardware design was also implemented. The Simulink model of a 1.7 kW bidirectional converter was verified using MATLAB output and the test results were compared with the hardware results. Compared to other bidirectional converter, use of DC-DC converter reduces the device losses dramatically and improves the converter efficiency. The bidirectional converter maintains an extremely high efficiency of above 80% over a wide range of output power in both forward and backward direction. The peak efficiency of the converter measured in both directions is 80%. The proposed high power bidirectional converter has achieved a power loss reduction. This has reduced the heat sink requirement and hence made the converter very compact in size.

REFERENCES

[1] Baliga B. J, (1982), "Semiconductors for high-voltage, vertical channel field effect transistors," Journal of Applied Physics, Vol. 53, pp.1759-1764.

[2] Carvalho Neto J. T and Salazar A. O. (2015), "One-Cycle Control applied to a bidirectional Buck-Boost converter in energy storage applications," *2015 IEEE 13th Brazilian Power Electronics Conference and 1st Southern Power Electronics Conference (COBEP/SPEC)*, Fortaleza, pp. 1-6.

[3] Chiu. H. J, Lin. L. W, (2006), 'A bidirectional DC-DC converter for fuel cell electric vehicle driving system,' IEEE Trans. Power Electron., Vol. 21, No. 4, pp.950 - 958.

[4] Dimna Denny C and Shahin M, (2015) 'Analysis of bidirectional SEPIC/Zeta converter with coupled inductor', *2015 International Conference on Technological Advancements in Power and Energy (TAP Energy)*, Kollam, pp. 103-108.

[5] Garcia-Rodriguez. L, Jones. V, Balda. J, Lindstrom. E, Oliva. A and Gonzalez-Llorente. J, (2014) 'Design of a GaN-based microinverter for photovoltaic systems,' 2014 IEEE International Symposium in Power Electronics for Distributed Generation Systems (PEDG).

[6] Ge. J, Zhao. Z, Ma. J, He. F, Yuan. L and Lu. T, (2014), 'Phase-shift control of isolated bidirectional DC-DC converters for unidirectional power flow,' *2014 IEEE Energy Conversion Congress and Exposition (ECCE)*, Pittsburgh, PA, pp. 1099-1104.

[7] Han. D, Noppakunkajorn. J and Sarlioglu. B, (2013), "Efficiency comparison of SiC and Si-based bidirectional DC-DC converters," *2013 IEEE Transportation Electrification Conference and Expo (ITEC)*, Detroit, MI, pp. 1-7.

[8] Hsieh Y. C., Chang Y. N., Lee K. Y., Chiu Y. C and Wu W. T, (2015) 'Bidirectional softly switched DC-to-DC converter with galvanic isolation,' *2015 IEEE International Conference on Industrial Technology (ICIT)*, Seville, pp. 952-956.

[9] Hui Li, Fang Zheng Peng and Lawler J. S, (2003) 'A natural ZVS medium-power bidirectional DC-DC converter with minimum number of devices,, in *IEEE Transactions on Industry Applications*, Vol. 39, No. 2, pp. 525-535.

[10] Hui Li, Peng F. Z and Lawler J. S, (2001), 'A natural ZVS high-power bi-directional DC-DC converter with minimum number of devices,' *Conference Record of the 2001 IEEE Industry Applications Conference. 36th IAS Annual Meeting (Cat. No.01CH37248)*, Chicago, IL, USA, pp. 1874-1881 Vol.3.

[11] Inoue. S, Akagi. H, (2007), 'A bidirectional DC–DC converter for an energy storage system with galvanic isolation,' IEEE Trans. Power Electron., Vol. 22, No. 6, pp.2299 -2306.

[12] Inoue. S, Akagi. H, (2007), 'A bi-directional isolated DC/DC converter as a core circuit of the next-generation medium-voltage power conversion system,' IEEE Trans. Power Electron., Vol. 22, No. 2, pp.535 - 542.

[13] Jiang. T, Zhang. J, Wu. X, Sheng. K, Wang. Y, (2015), 'A Bidirectional LLC Resonant Converter with Automatic Forward and Backward Mode Transition,' IEEE Transactions on Power Electronics, Vol.30, pp.757- 770.

[14] Jun Cai and Qing-Chang Zhong, (2014), 'Compact bidirectional DC-DC converters with two input sources,' *2014 IEEE 5th International Symposium on Power Electronics for Distributed Generation Systems (PEDG)*, Galway, pp. 1-5.

[15] Kaminski. N, (2009), 'State of the art and the future of wide band-gap devices,' in Proc. 13th European

Conference on Power Electronics and Applications, pp. 1-9.

[16] LaBella. T and Lai J. S, (2014) 'A Hybrid Resonant Converter Utilizing a Bidirectional GaN AC Switch for High-Efficiency PV Applications,' in *IEEE Transactions on Industry Applications*, Vol. 50, No. 5, pp. 3468-3475.

[17] Millan. J, Godignon. P, Perpina. X, Perez-Tomas Rebollo, A. J, (2014), 'A survey of wide bandgap power semiconductor devices,' IEEE Trans. On Power Electronics, Vol. 29, pp. 2155– 2163.

[18] Miura. Y, Kaga. M, Horita. Y and Ise. T, (2010), 'Bidirectional isolated dual full-bridge DC-DC converter with active clamp for EDLC,' in Proc. IEEE Energy Convers. Congr. Expo, pp. 1036–1143.

[19] Miura. Y, Kaga. M, Horita. Y and Ise. T, (2010), 'Bidirectional isolated dual full-bridge DC-DC converter with active clamp for EDLC,' Proc. IEEE Energy Convers. Congr. Expo, pp.1036-1143.

[20] Moses M. B and Banu J. B. (2015), 'A new isolated bidirectional full bridge buck-boost converter with LCD clamp circuit, *2015 IEEE Conference on Energy Conversion (CENCON)*, Johor Bahru, pp. 25-30.

[21] Nymand. M, Andersen. M. A. E, (2010), 'High-efficiency isolated boost DC-DC converter for high-power low-voltage fuel cell applications,' IEEE Trans. Ind. Electron., Vol. 57, No. 2, pp. 505-514.

[22] Panov. Y, Jovanovic. M. M, Gang. L and Yueyong. M, (2014), 'Transformer-flux-balancing control in isolated bidirectional DC-DC converters,' *2014 IEEE Applied Power Electronics Conference and Exposition - APEC 2014*, Fort Worth, TX, pp. 49-56.

[23] Ramachandran. R, Nymand. M, (2015), 'Design and Analysis of an Ultra-High Efficiency Phase Shifted Full Bridge GaN Converter,' Applied Power Electronics Conference and Exposition, 30th Annual APEC Conference Proceedings 2015, pp.2011-2016.

[24] Ramachandran. R, Nymand. M, Petersen. N. H, (2014), 'Design of a compact, ultra -high efficient isolated DC-DC converter utilizing GaN devices,' Industrial Electronics Society, IECON 2014 - 40th Annual Conference of the IEEE, Vol., No., pp.4256-4261.

[25] Ugur. E and Vural. B, (2014), 'Comparison of different small signal modeling methods for bidirectional DC-DC converter,' *2014 International Conference on Renewable Energy Research and Application (ICRERA)*, Milwaukee, WI, pp. 913-915.